AD-A035 909 NAVAL POSTGRADUATE SCHOOL MONTEREY CALIF F/G 1/1
DEVELOPMENT OF A CONTROL VALVE TO INDUCE AN OSCILLATING BLOWING--ETC(U)
DEC 76 J L BAUMAN
UNCLASSIFIED NL

1 OF 1
AD-A
035909

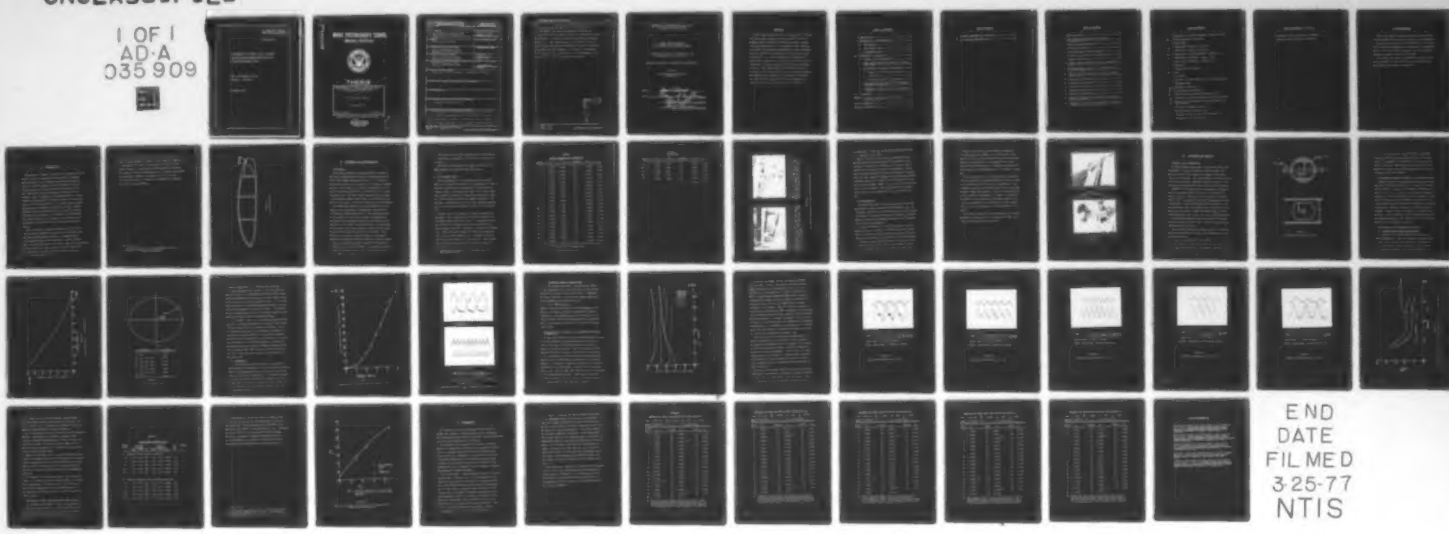

END
DATE
FILMED
3-25-77
NTIS

U.S. DEPARTMENT OF COMMERCE
National Technical Information Service

AD-A035 909

DEVELOPMENT OF A CONTROL VALVE TO INDUCE AN OSCILLATING BLOWING COEFFICIENT IN A CIRCULATION CONTROL ROTOR

NAVAL POSTGRADUATE SCHOOL
MONTEREY, CALIFORNIA

DECEMBER 1976

NAVAL POSTGRADUATE SCHOOL
Monterey, California

THESIS

DEVELOPMENT OF A CONTROL VALVE TO INDUCE AN OSCILLATING BLOWING COEFFICIENT IN A CIRCULATION CONTROL ROTOR

by

James Lawrence Bauman

December 1976

Thesis Advisor: J. A. Miller

SECURITY CLASSIFICATION OF THIS PAGE (When Data Entered)

REPORT DOCUMENTATION PAGE		READ INSTRUCTIONS BEFORE COMPLETING FORM
1. REPORT NUMBER	2. GOVT ACCESSION NO.	3. RECIPIENT'S CATALOG NUMBER
4. TITLE (and Subtitle) Development of a Control Valve to Induce an Oscillating Blowing Coefficient in a Circulation Control Rotor		5. TYPE OF REPORT & PERIOD COVERED Master's Thesis December 1976
		6. PERFORMING ORG. REPORT NUMBER
7. AUTHOR(s) James Lawrence Bauman		8. CONTRACT OR GRANT NUMBER(s)
9. PERFORMING ORGANIZATION NAME AND ADDRESS Naval Postgraduate School Monterey, California 93940		10. PROGRAM ELEMENT, PROJECT, TASK AREA & WORK UNIT NUMBERS
11. CONTROLLING OFFICE NAME AND ADDRESS Naval Postgraduate School Monterey, California 93940		12. REPORT DATE December 1976
		13. NUMBER OF PAGES 51
14. MONITORING AGENCY NAME & ADDRESS(if different from Controlling Office) Naval Postgraduate School Monterey, California 93940		15. SECURITY CLASS. (of this report) Unclassified
		15a. DECLASSIFICATION/DOWNGRADING SCHEDULE

16. DISTRIBUTION STATEMENT (of this Report)

Approved for public release; distribution unlimited.

17. DISTRIBUTION STATEMENT (of the abstract entered in Block 20, if different from Report)

18. SUPPLEMENTARY NOTES

19. KEY WORDS (Continue on reverse side if necessary and identify by block number)

circulation control rotor

20. ABSTRACT (Continue on reverse side if necessary and identify by block number)

The Circulation Control Rotor concept makes it possible to achieve large changes in lift coefficient, without changing angle of attack, by making only small changes in blowing coefficient. The concept has great potential

in the area of rotary-wing aerodynamics, where implementation will require the generation of oscillating blowing coefficients. In order to examine the response of a circulation control airfoil to such an oscillating blowing coefficient, a simple control valve system was designed and built. The effectiveness of the control valve in oscillating the blowing coefficient at various frequencies and amplitudes was examined. An attempt to determine the effect of this oscillation on the instantaneous lift coefficient of the rotor was not successful.

Development of a Control Valve to Induce an
Oscillating Blowing Coefficient in a
Circulation Control Rotor

by

James Lawrence Bauman
Lieutenant, United States Navy
B.S., Iowa State University, 1970

Submitted in partial fulfillment of the
requirements for the degree of

MASTER OF SCIENCE IN AERONAUTICAL ENGINEERING

from the

NAVAL POSTGRADUATE SCHOOL
December 1976

Author James L Bauman

Approved by: ______ Thesis Advisor

______ Chairman, Department of Aeronautics

______ Dean of Science and Engineering

ABSTRACT

The Circulation Control Rotor concept makes it possible to achieve large changes in lift coefficient, without changing angle of attack, by making only small changes in blowing coefficient. The concept has great potential in the area of rotary-wing aerodynamics, where implementation will require the generation of oscillating blowing coefficients. In order to examine the response of a circulation control airfoil to such an oscillating blowing coefficient, a simple control valve system was designed and built. The effectiveness of the control valve in oscillating the blowing coefficient at various frequencies and amplitudes was examined. An attempt to determine the effect of this oscillation on the instantaneous lift coefficient of the rotor was not successful.

TABLE OF CONTENTS

LIST OF TABLES

LIST OF FIGURES

LIST OF SYMBOLS

A	Area open to air flow through the control valve.
A_s	Trailing edge slot exit area.
c	Chord length
C_D	Coefficient of Drag, $(2\ D)/(q\ S)$
C_L	Coefficient of Lift, $(2\ L)/(q\ S)$
C_M	Coefficient of Pitching Moment, $(2M)/(q\ S\ c)$
C_P	Coefficient of Pressure, $(P_{tap} - P_o)/q$
C	Coefficient of Blowing, $(m\ V_j)/(q\ S)$
D	Drag Force
H	Control Valve Cam Radius
Hz	Hertz
L	Lift Force
m	Air mass flow rate through the trailing edge slot.
M	Pitching Moment
P_{atm}	Atmospheric Pressure
P_I	Internal Plenum Pressure
P_I'	(RMS of plenum oscillation amplitude)/(P_I)
P_{tap}	Pressure at a given pressure tap on model surface.
P_{22}'	(RMS of Tap 22 pressure oscillation)/(mean Tap 22 pressure)
q	Wind tunnel dynamic pressure
S	Airfoil planform surface area
V_j	Velocity of air jet from trailing edge slot
w	Frequency of C_μ oscillations

LIST OF SYMBOLS (continued)

X	Horizontal airfoil reference coordinate
Y	Vertical airfoil reference coordinate

ACKNOWLEDGEMENT

The author wishes to thank Professor James A. Miller for his guidance and assistance during this investigation.

Recognition is also due to Professor Louis V. Schmidt for his advice and suggestions, and Messrs. Glen Middleton and John Moulton for their valuable technical assistance during the construction of the equipment.

The author also wishes to express his special thanks and appreciation to his wife, Clare, whose support and encouragement were deeply appreciated.

I. INTRODUCTION

References 1 through 4 report that the method of circulation control by tangential blowing over the rounded trailing edge of an elliptical airfoil can be used to achieve a large increase in lift coefficient with only a small increase in blowing momentum coefficient, C_μ. The tangential blowing increases the momentum of the boundary layer, causing the aft separation point to move along the trailing edge toward the bottom of the airfoil. Because of the Coanda effect, the boundary layer remains attached and the separation point can in fact be moved forward along the lower surface of the airfoil, greatly increasing the circulation. Therefore, by controlling the blowing velocity it is possible to control the lift generated by the airfoil without changing the angle of attack.

This concept has possible application in the field of helicopter aerodynamics, where each rotor blade must constantly change angle of attack to compensate for both unsteady relative wind and cyclic control inputs. Since the lift generated by the rotor blade can be controlled by adjusting the blowing velocity, cyclic control can be implemented by means of modulating the air supply to the trailing edge jet.

The simplest cyclic control signal is a sinusoidal input whose frequency is equal to the rotational frequency of the main rotor shaft. Development of such a control would require a sinusoidally oscillating blowing velocity. The purpose of this investigation was to design and assemble the necessary hardware to generate a C_μ[1] of the form $A + B \sin (wt)$ and, if possible, investigate the response of C_L to the oscillating C_μ.

---

[1]Blowing velocity, V_j, is non-dimensionalized to coefficient of blowing, C_μ, defined as:

$$C_\mu = (m V_j)/(q S)$$

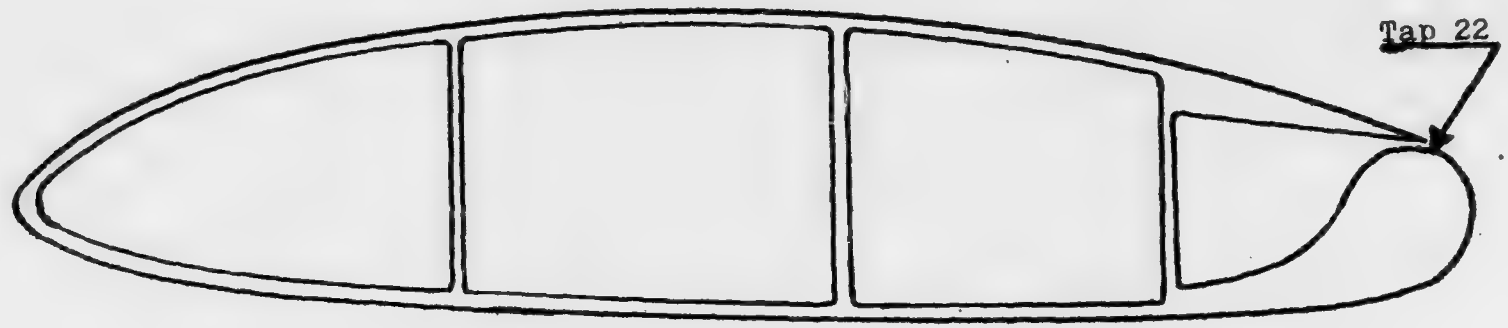

Figure 1

Airfoil Section

II. EQUIPMENT AND INSTRUMENTATION

A. THE AIRFOIL

The airfoil used was a prototype section obtained from the Lockheed Phase I Study on Circulation Control Rotor (CCR) design feasibility [Ref. 4]. It was an elliptical section with a chord of 10.2 inches, thickness ratio of 0.20, camber of 3.3%, and incorporated a slot near the trailing edge at $X/C = 0.95$; Fig. 1 is a cross-sectional view. The slot width was adjustable by means of jack screws located about every two inches along the span, and was set at 0.010 inch throughout the investigation.

The model was mounted in the oscillating flow wind tunnel in the Department of Aeronautics Laboratories at the Naval Postgraduate School. The oscillating mode of the tunnel is to be used in later investigations; this current investigation employed only steady tunnel velocities. The tunnel test section was 24 inches square and the model, which was slightly longer than 24 inches, extended through the side walls of the tunnel. The portion of the model's trailing edge slot extending outside the tunnel was securely sealed to prevent leakage.

Air for the trailing edge blowing was provided by a plenum cavity inside the model; the plenum was supplied by means of one-and-one-half inch steel pipes attached to both ends of the model.

The airfoil contained 53 pressure taps located along the chord line at mid-span; location of the taps is given in Table I.

The model was mounted at an angle of attack of -5°, approximately the zero-lift angle of attack.

B. THE CONTROL VALVE

The air pressure in the plenum cavity inside the model was controlled by means of a rotating valve (Fig. 2a). The valve consisted of an elliptical Lucite cam which rotated inside a two-inch steel pipe. The cam was carefully shaped to provide a cross-section area which varied as a sine function of twice its angular position. The maximum cross-section area of the valve was approximately equal to the total exit area of the slot in the airfoil, A_s.[2]

A globe valve was installed in the air supply line upstream of the rotating valve to provide control over the maximum mass flow rate of air. A second globe valve was installed in a bypass line around the rotating control valve (Fig. 2a) to provide a steady flow component to C_μ. This valve also served to modify the amplitude of the oscillating component. C_μ, therefore, could be a function of the form $C_\mu = A + B \sin(wt)$, where A and B could be adjusted by means of the two globe valves.

---

[2]Suggested by Reader to be an optimum area ratio for oscillating C_μ [Ref. 5].

TABLE I

AIRFOIL PRESSURE TAP LOCATIONS

Tap #	X	Y	Tap #	X	Y
1	0.000	0.000	22	9.964	0.440
2	0.009	0.050	23	10.070	0.340
3	0.055	0.135	24	10.070	0.220
4	0.123	0.220	25	10.191	0.147
5	0.211	0.305	26	10.199	0.073
6.	0.327	0.400	27	10.215	0.000
7.	0.525	0.518	28	10.206	0.020
8.	0.954	0.710	29	10.162	0.040
9.	1.441	0.875	30	10.118	0.152
10.	1.931	1.004	31	10.051	0.255
11.	2.435	1.066	32	9.940	0.372
12.	2.851	1.182	33	9.800	0.400
13.	3.958	1.315	34	9.613	0.443
14.	5.086	1.360	35	9.114	0.525
15.	6.096	1.343	36	8.587	0.590
16.	7.132	1.238	37	7.960	0.638
17.	7.627	1.162	38	7.570	0.658
18.	8.019	1.088	39	7.059	0.678
19.	8.635	0.950	40	6.033	0.700
20.	9.028	0.844	41	5.116	0.708
21.	9.430	0.552	42	4.019	0.695

X in inches aft of leading edge.

Y in inches from chord line.

TABLE I
(continued)

Tap #	X	Y	Tap #	X	Y
43	2.902	0.665	48	0.521	0.388
44	2.496	0.645	49	0.349	0.320
45	1.992	0.610	50	0.230	0.260
46	1.478	0.560	51	0.115	0.178
47	0.964	0.490	52	0.034	0.098
			53	0.010	0.052

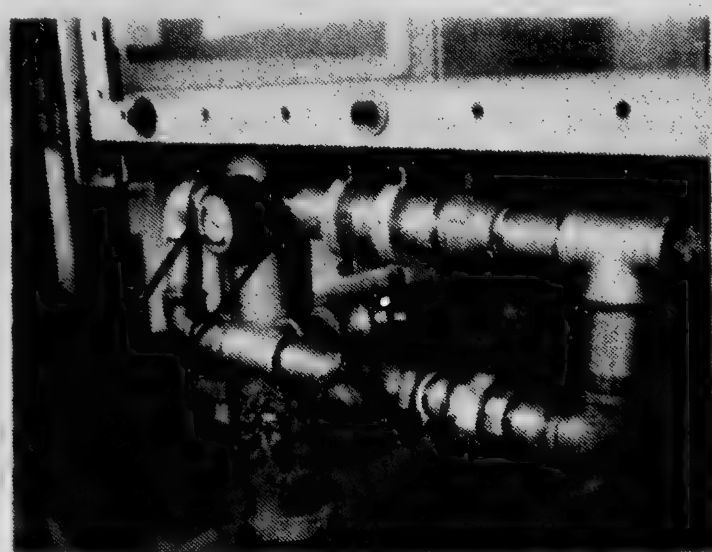

Figure 2a. Air enters through the rubber hose section at the rear. The rotating control valve is in the upper left corner and the bypass globe valve is in the lower center. Air exits at the right and is then ducted to the airfoil.

Figure 2b. Air comes up from the lower right, through the flowmeter (or the bypass line), through the master throttle globe valve (center) and exits to the control valve assembly at the rear.

Figure 2

Air Supply Plumbing and Control Valve Installation

The frequency, w, was set by driving the rotating valve with a variable speed motor.

Most of the air supply line was constructed from one-and-one-half inch steel pipe using standard pipe fittings. Several short sections of two-inch rubber suction hose were used to facilitate assembly. Rigid steel pipe was selected in order to eliminate the possibility of pipe diameter changes with oscillating pressure. No attempt was made to reduce the turbulence inside the pipe due to fittings, bends, etc., as this was considered to be a minor problem. Pipe length from the rotating control valve to the entrance of the airfoil was 13 feet.

C. INSTRUMENTATION

The mass flow rate of the air supplied to the model was measured using a variable area flowmeter (Fig. 2b). To prevent distortion of the flow pattern due to excessive oscillation of the meter during low frequency operations, provision was made to bypass the meter once the maximum flow rate had been adjusted.

A photosensitive cell, mounted behind a partially masked Lucite disc (Fig. 3) which was rotated in phase with the valve, provided a string of pulses which were counted to determine the frequency of the rotating valve.

Pressure lines from the 53 taps on the airfoil were connected to one of two scanivalves located on either end of the model (Fig. 4). In addition, each scanivalve

received P_o, P_T and P_{atm} for calibration purposes. The scanivalves were capable of selecting one input pressure line at a time and outputting a voltage proportional to the pressure on the selected line. This voltage was then displayed on a digital voltmeter, an oscilloscope, a true RMS meter and, if desired, a phasemeter.

For low values of C_μ it was possible to determine the air pressure in the plenum cavity directly by means of a pressure line into one of the scanivalves, but at higher values of C_μ (greater than 0.035) the plenum pressure became high enough to exceed the capabilities of the scanivalve transducer. In order to determine the shape of the oscillations at higher values of C_μ, a hot wire anemometer was inserted in the air supply line at a point determined to be least subject to turbulence.

The plenum pressure was also connected to a mercury manometer, which was used to determine the mean value of the oscillating plenum pressure.

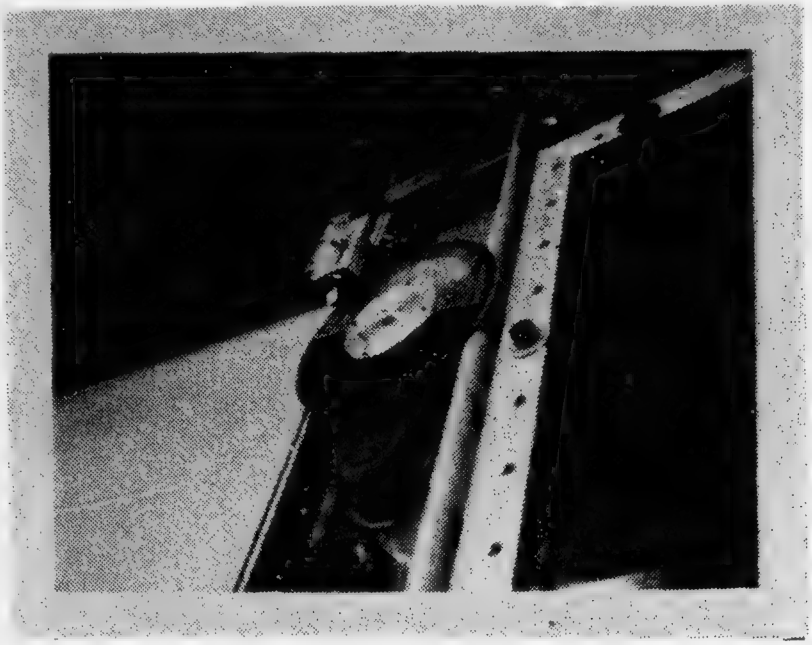

Figure 3
Control Valve RPM Detector

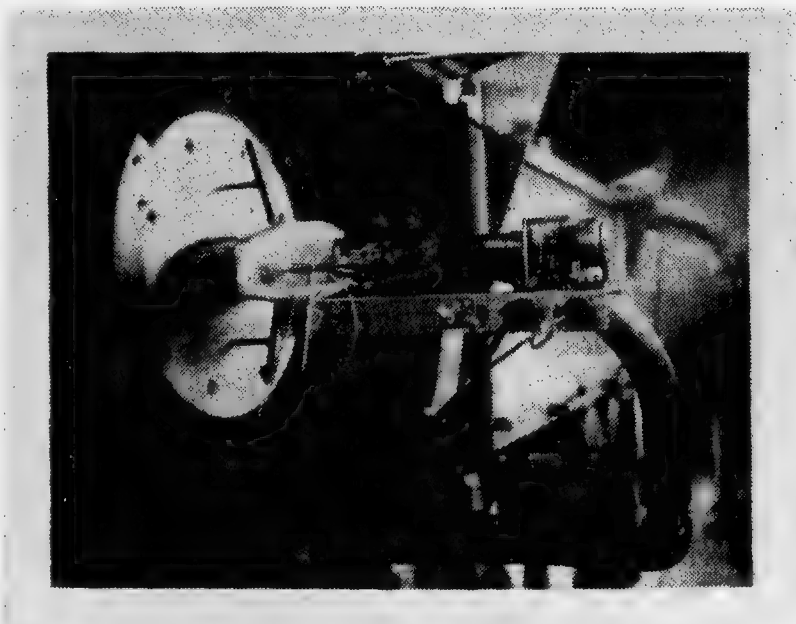

Figure 4
Scanivalve Mount

III. PROCEDURES AND RESULTS

A. CONTROL VALVE CONSTRUCTION

Several attempts were made to develop a simple, easy-to-construct control valve which would modulate the mass flow rate of the plenum air supply in something close to a sine wave. The first attempts utilized rotating flat discs of various diameters inside the pipe. These all produced oscillations which were far from sinusoidal.

Reference 5 indicated that the maximum cross-section area of the valve should be close to the total exit area of the slot. The total exit area was 0.24 square inches, which indicated that a three-dimensional cam would be required to achieve the desired flow modulation. It was determined that the simplest way to meet this requirement was to construct a sphere of radius equal to the internal radius of the pipe. The sphere was then mounted on a shaft which passed through the center of the pipe and was modified in such a way to provide a sinusoidally varying area for the valve.

For a sphere modified as shown in Fig. 5, the cross-section area available for air flow (shaded area) in the position shown is:

$$A = 2\,[\sin^{-1}(1-H^2)^{\frac{1}{2}} - H(1-H^2)^{\frac{1}{2}}]$$

Since the area is to vary sinusoidally as the cam rotates, H must vary as a function of cam angular position, θ, such

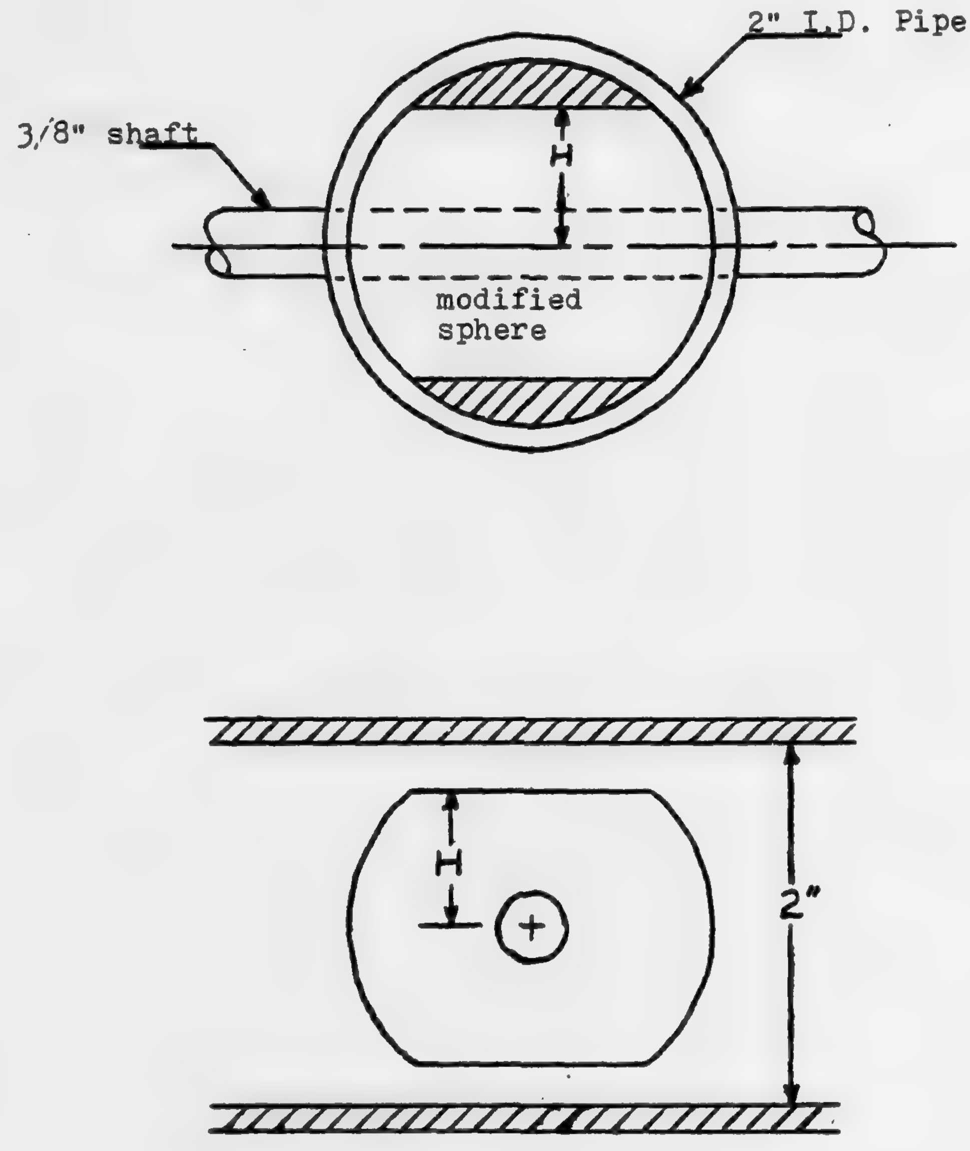

Figure 5

Rotating Control Valve Concept

that:

$$A = A_s \left|\sin \theta\right| = 2\left[\sin^{-1}(1-H^2)^{\frac{1}{2}} - H(1-H^2)^{\frac{1}{2}}\right]$$

Figure 6 shows how the area varies with H. From this curve it is possible to determine H for any value of θ. Figure 7 shows the final shape of the cam. Due to the symmetrical shape, air flow modulation was at twice the frequency of the cam rotation.

B. MEAN PLENUM PRESSURE RESPONSE TO AIR MASS FLOW RATE

Figure 8 shows the relationship between mean plenum pressure and rotameter reading. The data points shown were recorded at 15.2 Hz, but subsequent measurements taken at 10.0, 7.0, 5.1 and 3.6 Hz showed no frequency dependence in the relationship. All data points, regardless of frequency, were very near the indicated line. Low frequency operation caused the rotameter to oscillate considerably, making it difficult to obtain accurate readings. Figure 8 made it possible to determine the mean value of $\dot{m}$ by reading the mean plenum pressure from the mercury manometer. The manometer was not noticeably affected by the pressure variations.

C. EVALUATION OF THE PRESSURE OSCILLATIONS

1. Shape of the Plenum Pressure Wave

The air foil plenum cavity was attached to a mercury manometer in order to determine the mean plenum pressure, but no means was available to determine the actual fluctuating pressure (except at very low values of C_μ, when the pressure was within the range of the

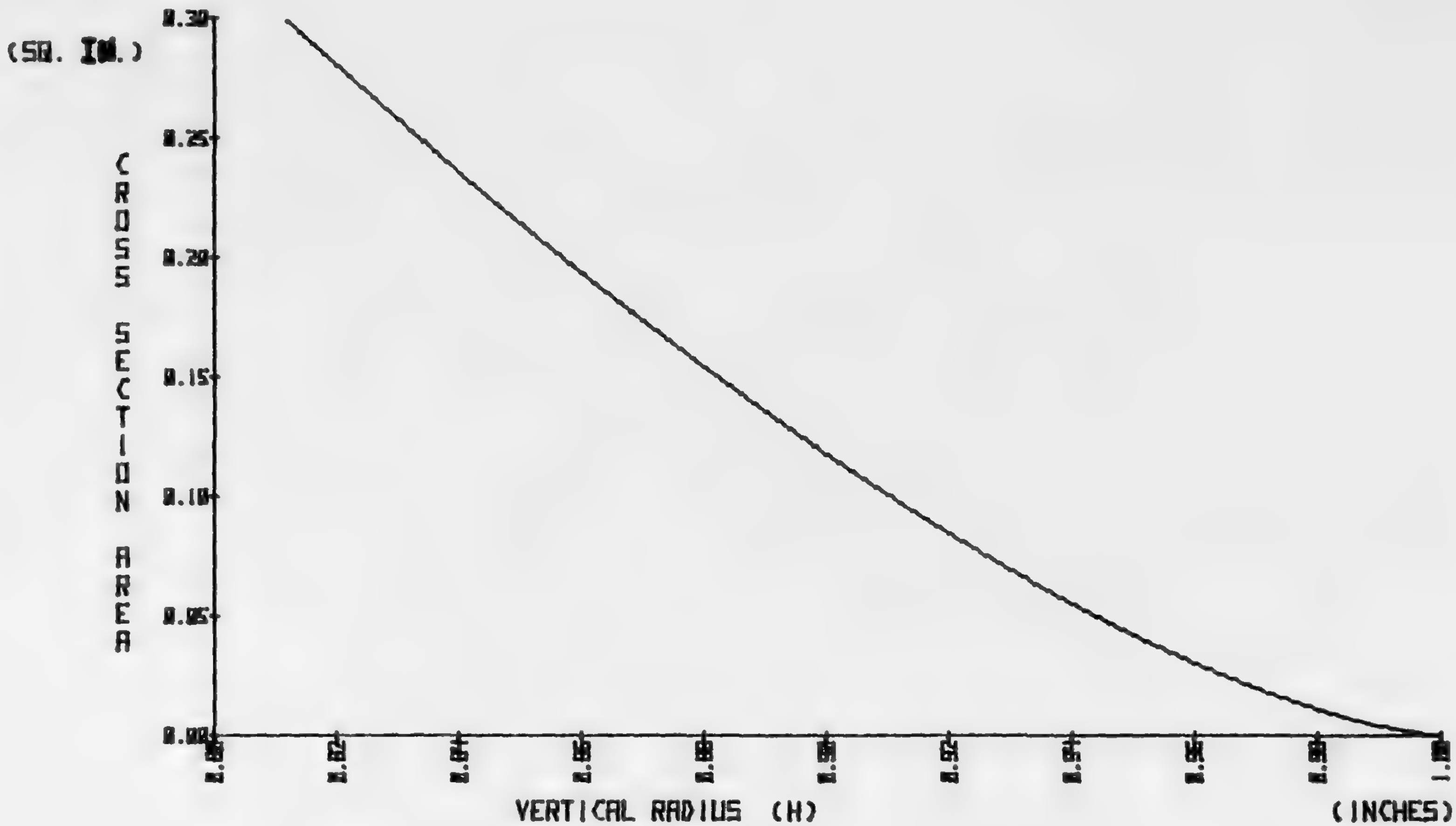

Figure 6

Control Valve Area vs. Cam Radius (H)

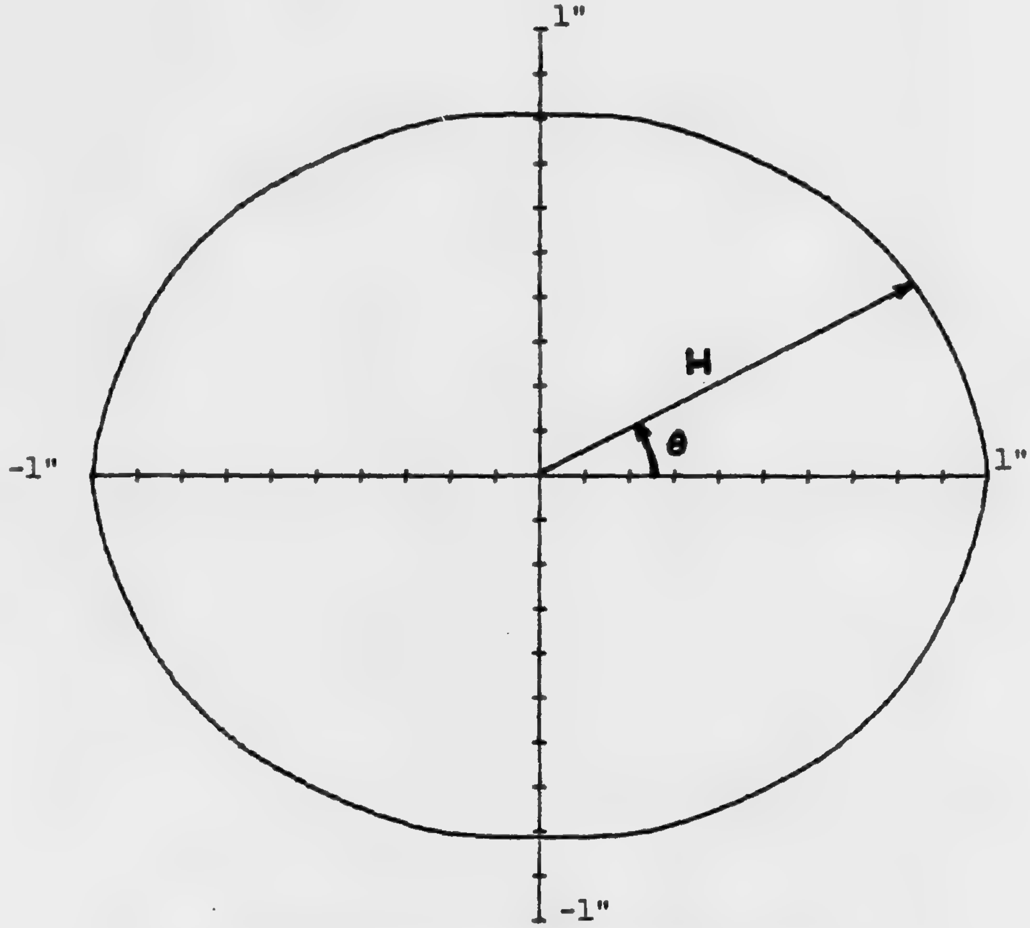

θ (degrees)	(inches)
0, 180	1.000
15, 165, 195, 345	0.918
30, 150, 210, 330	0.930
45, 135, 225, 315	0.888
60, 120, 240, 300	0.853
75, 105, 255, 285	0.829
90, 270	0.812

Figure 7

Section View of Cam

scanivalve transducer). To overcome this problem, a hot wire anemometer was placed in the air supply line. Figure 9 shows the correspondence between actual plenum pressure (upper trace) and hot wire output (lower trace) at 3.6 Hz and 10.0 Hz at low values of C_μ. It is evident that the shape of the plenum pressure variation is very close to the shape of the hot wire output. The traces are of opposite polarity since the plenum pressure signal underwent a sign inversion during processing.

As shown in Fig. 8, for rotameter readings greater than 0.20, the plenum pressure was linearly proportional to the air mass flow rate (rotameter reading). Since air mass flow rate was in turn assumed proportional to the velocity through the pipe, it was further assumed that the hot wire anemometer, which measured the velocity, was proportional to the plenum pressure. This linear relationship does not hold for rotameter readings below 0.20, but flow rates this low are of little practical value due to the very low values of C_μ generated (of the order 0.01).

2. Distortion

The distortion shown in Fig. 9b, consisting of a small peak which appeared as the velocity was decreasing, showed up during operations at low values of C_μ, particularly at the higher frequencies. The cause is unknown, but it may have been a reverse flow brought on by the closing valve. The value of C_μ used for Fig. 9 was quite low; for values of C_μ of practical interest, the distortion was considerably smaller.

Figure 8

Plenum Pressure Variation With Air Mass Flow Rate

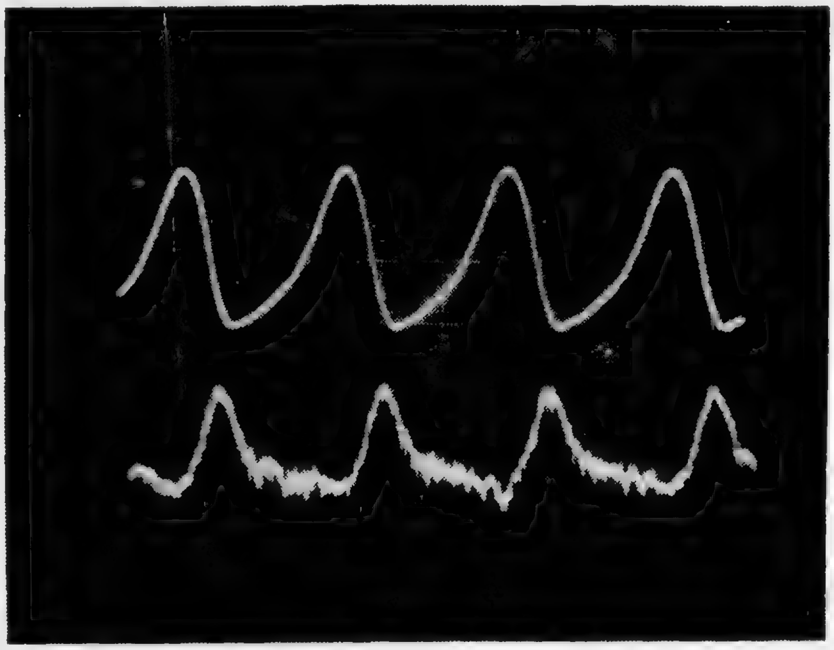

Figure 9a. 3.6 Hz.

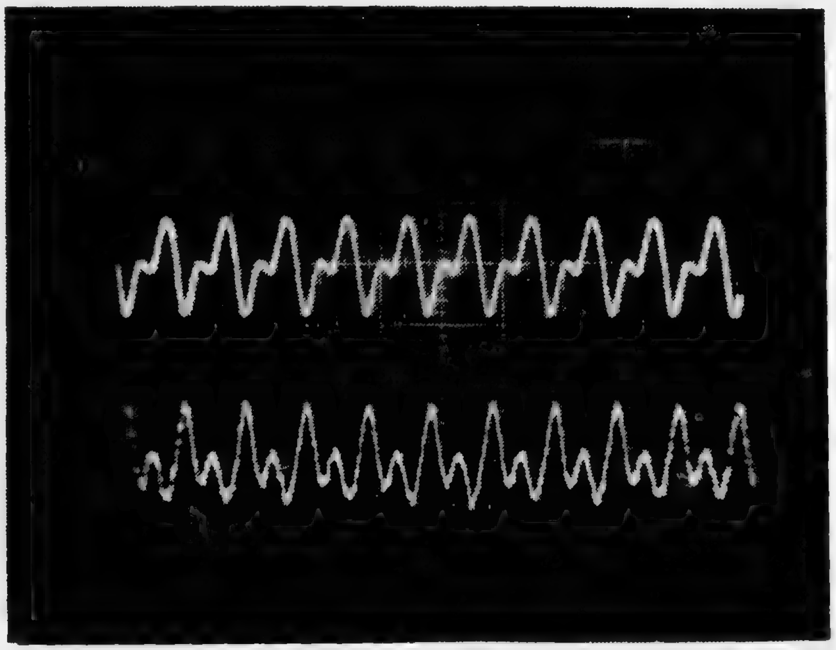

Figure 9b. 10.0 Hz.

Upper Trace -- Plenum Pressure
Lower Trace -- Hot Wire Anemometer in Air Supply Line

NOTE: Amplitudes are of different scales.

Figure 9

Correspondence Between Plenum Pressure and Hot Wire Signal

3. Frequency Effects on Amplitude

An attempt was made to determine what effect, if any, frequency had on the amplitude of the pressure oscillation created by the control valve. Amplitude was recorded as RMS of the hot wire signal expressed as a percentage of the mean value, or:

$$P_I' = (RMS)(100)/(P_I)$$

Figure 10 shows the results of the investigation. In general, increasing frequency increased the percent oscillation, but changing C_μ had little effect. The values recorded were the maximum amplitude attainable; that is, the bypass line around the control valve was fully closed.

D. EVALUATION OF THE EFFECTS ON THE EXTERIOR PRESSURE DISTRIBUTION

It was anticipated that the fluctuating plenum pressure, P_I', would generate an oscillating C_μ which would, in turn, creat observable oscillations in the surface pressure around the airfoil. This fluctuating surface pressure distribution would then cause C_L to oscillate.

To investigate how effective the oscillating plenum pressure was in generating oscillations in the surface pressure, the pressure signal from each of the 53 taps was displayed on an oscilloscope. Except for the taps very close to the trailing edge jet, there was very little change in the pressure distribution. Even tap 22, which was immediately behind the slot, showed oscillation amplitude considerably smaller than expected. Figures 11, 12, 13,

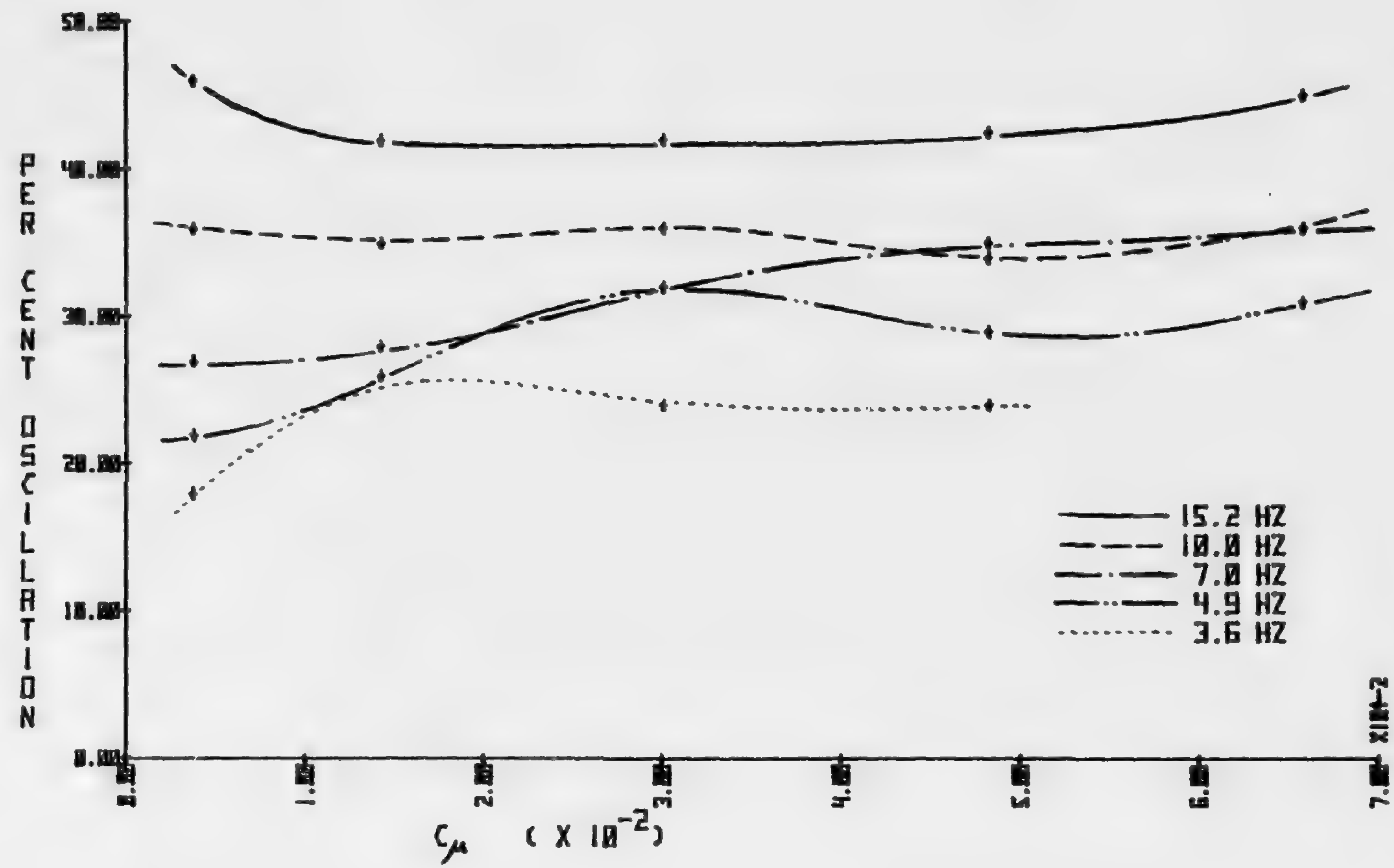

Figure 10

Effect of C_μ and Frequency on Plenum Pressure Oscillation

14 and 15 show the shape of both the plenum pressure wave (actually, the hot wire signal) and the pressure signal from tap 22 at frequencies of 3.6, 5.1, 7.0, 10.0 and 15.1 Hz respectively. These pictures were taken at maximum plenum pressure amplitude; reducing the amplitude caused the tap 22 pressure amplitude to decrease as well, but did not significantly change the shape of the signal. Table II lists the values of the steady and fluctuating (RMS) components of each signal, both at maximum plenum pressure amplitude and with plenum amplitude reduced to one-half of maximum. As in Fig. 10, the "size" of the oscillation was determined by expressing the RMS value of the signal as a percentage of the steady value; this gave values of plenum percentage oscillation, P'_I, and tap 22 percentage oscillation, P'_{22}.

The ability of the oscillating plenum pressure to induce oscillations in the exterior surface pressure was measured by taking the ratio of P'_{22}/P'_I; this showed how a given percentage pressure change in the plenum affected the surface pressure. In this way, the effect of frequency on the ability to induce surface pressure oscillations could be determined without correcting for frequency effects on plenum pressure amplitude (as shown in Fig. 10).

Figure 16 shows these results at both plenum signal amplitudes. The effect of frequency decreased significantly at about 7 Hz. It was assumed that the ratio of P'_{22}/P'_I would continue to rise as frequency decreased below

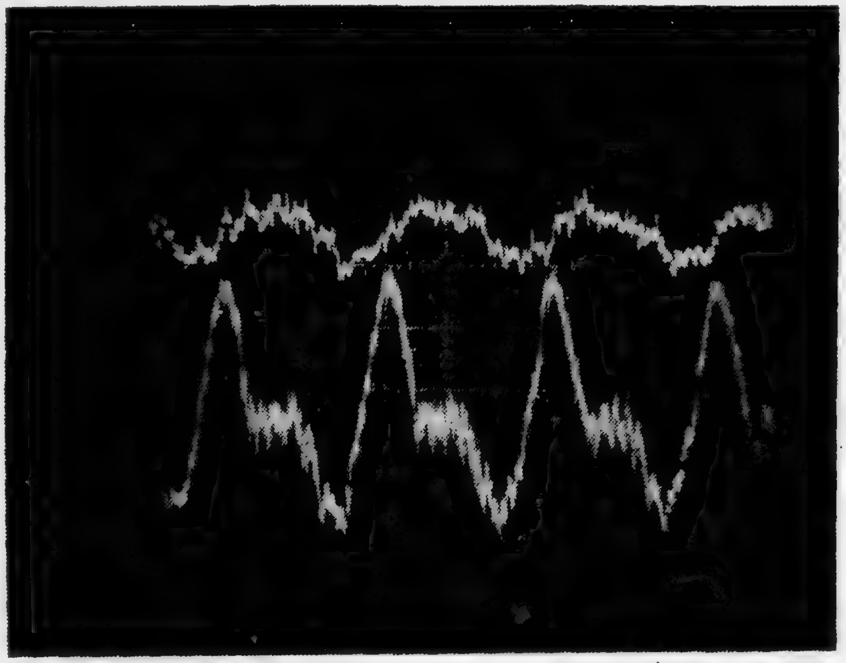

Upper Trace -- Surface Pressure Just Behind the Trailing Edge Jet (Tap 22)

Lower Trace -- Plenum Pressure

NOTE: Amplitudes on different scales.

Figure 11

Pressure Oscillations at 3.6 Hz.

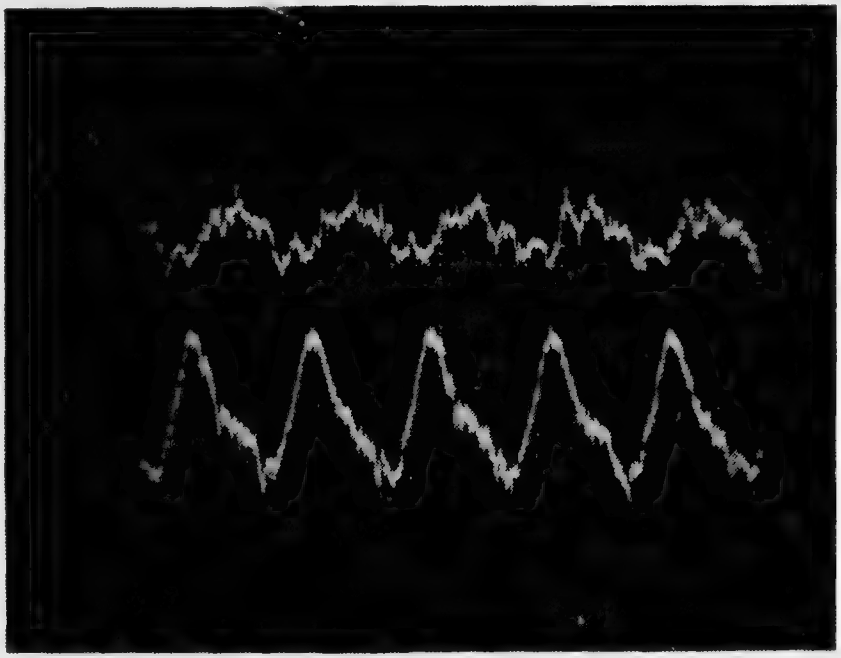

Upper Trace -- Surface Pressure Just Behind Trailing Edge Jet. (Tap 22)

Lower Trace -- Plenum Pressure.

NOTE: Amplitudes on different scales.

Figure 12

Pressure Oscillations at 5.1 Hz.

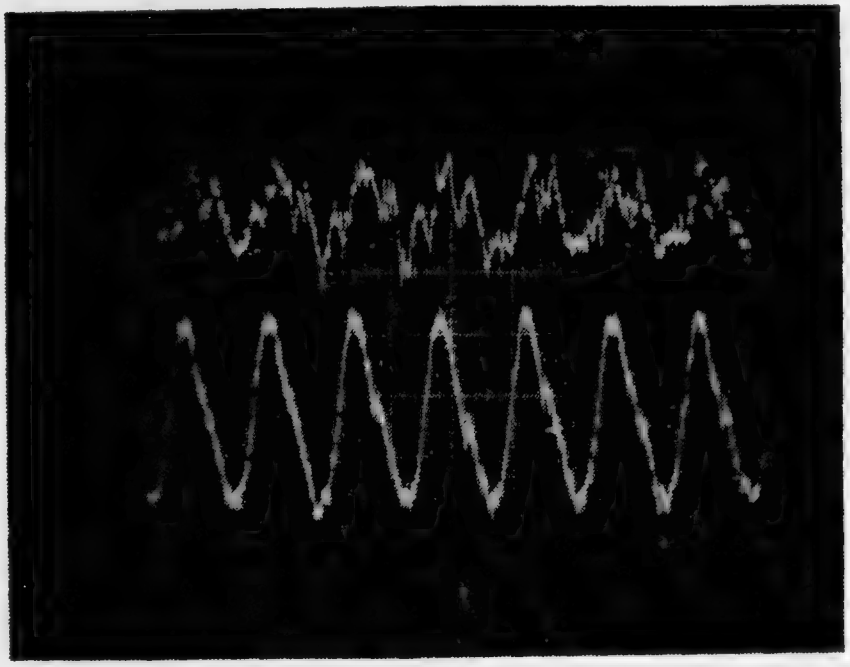

Upper Trace -- Surface Pressure Just Behind
Trailing Edge Jet. (Tap 22)

Lower Trace -- Plenum Pressure.

NOTE: Amplitudes on different scales.

Figure 13

Pressure Oscillations at 7.0 Hz.

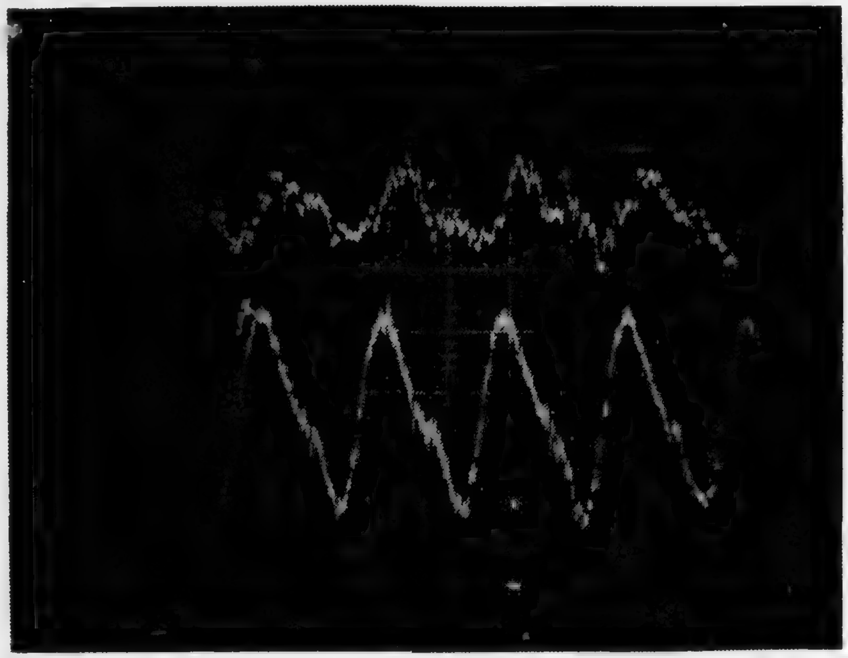

Upper Trace -- Surface Pressure Just Behind Trailing Edge Jet. (Tap 22)

Lower Trace -- Plenum Pressure.

NOTE: Amplitudes on different scales.

Figure 14

Pressure Oscillations at 10.0 Hz.

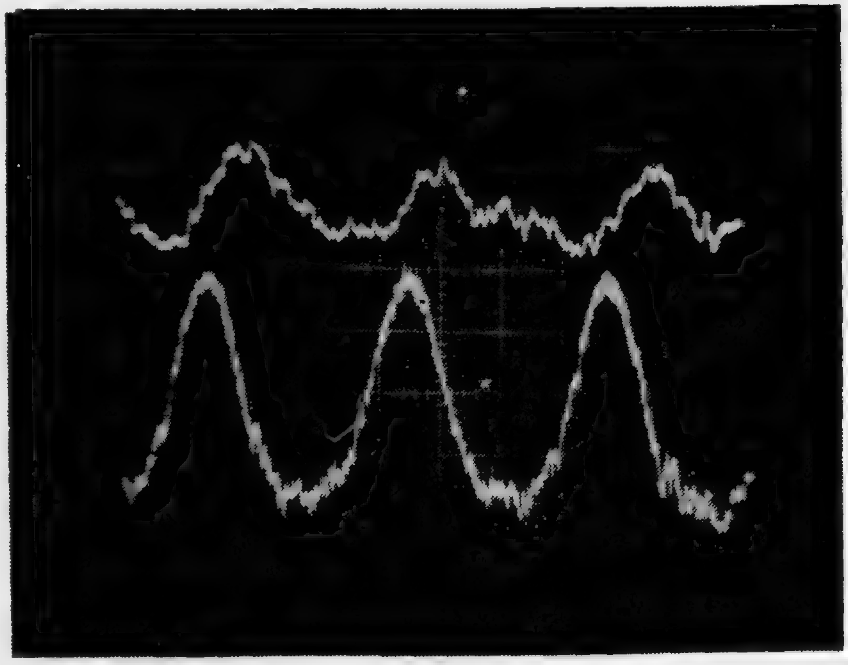

Upper Trace -- Surface Pressure Just Behind Trailing Edge Jet. (Tap 22)

Lower Trace -- Plenum Pressure.

NOTE: Amplitudes on different scales.

Figure 15

Pressure Oscillations at 15.1 Hz.

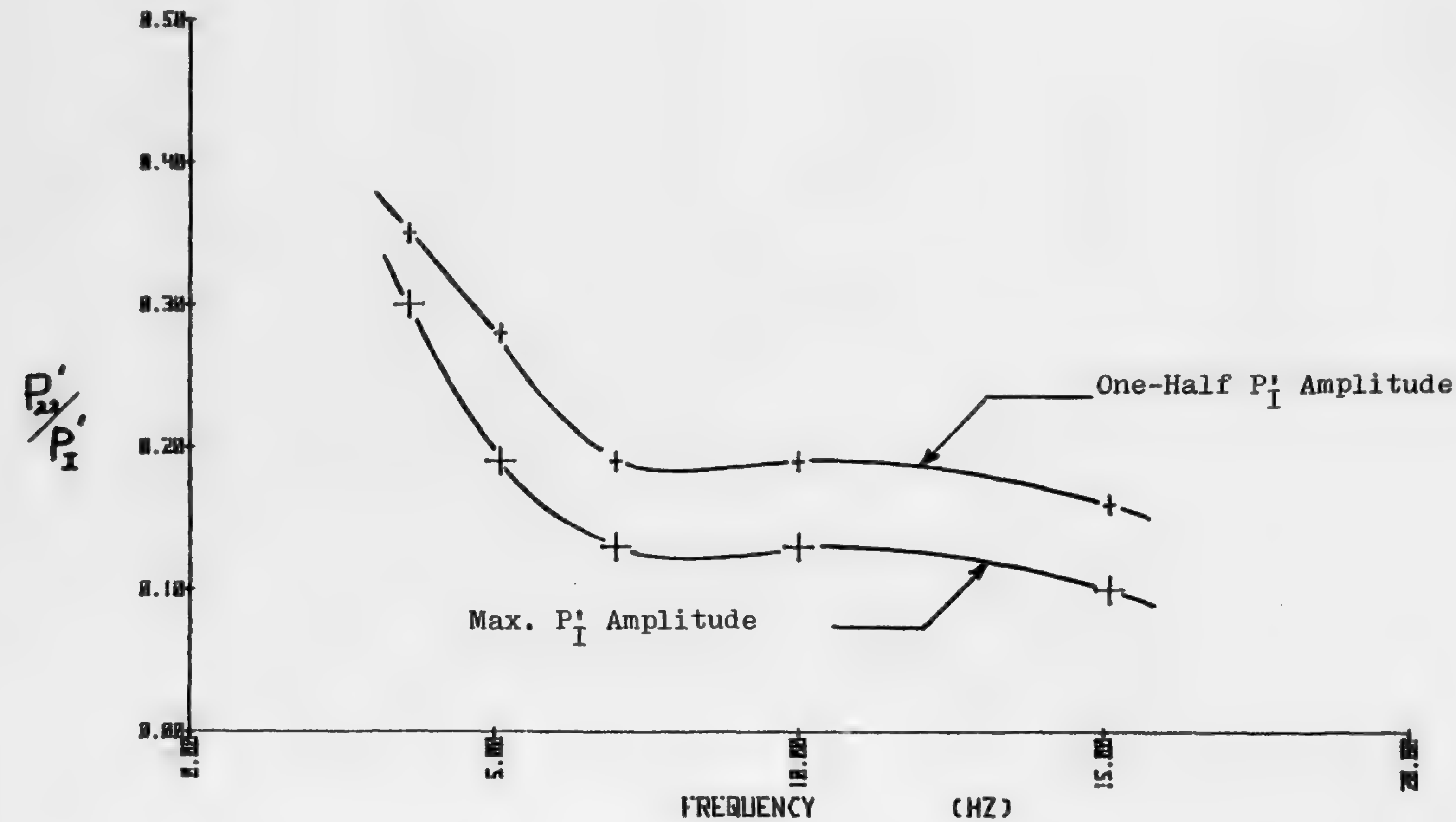

Figure 16

Effect of Frequency on Amplitude Loss Across the Trailing Edge Jet

3.6 Hz. since at very low frequencies a quasi-steady condition results which would bring the ratio very close to 1.0. Above 7 Hz., increasing the frequency had a very slight degrading effect on signal propagation.

It is interesting to note that when the plenum pressure amplitude was reduced to one-half the maximum value, the ratio increased significantly. Table II shows that this was the result of the fact that the RMS of the surface pressure signal did not decrease proportionately with the plenum pressure RMS.

Figures 11 through 15 show that the surface pressure oscillation lagged behind the plenum pressure as expected; rough measurements from the pictures indicate the phase lag was about 50-70 degrees, but the large turbulence effects in the surface signal made accurate measurement impossible.

The pressure oscillation evident at tap 22 rapidly decayed as it moved around the trailing edge. At tap 24, about one-quarter inch behind tap 22, the oscillation had already disappeared into the turbulence noise. The remaining taps showed little or no effect from the oscillating C_μ.

E. COMPARISON OF MEAN VALUE DATA WITH STEADY C_μ DATA

To determine what effect, if any, the oscillating C_μ had on the mean value of C_L, five complete sets of pressure tap data (see Appendix) were taken at various C_μ frequencies and amplitudes. The results of these

TABLE II

OSCILLATING PRESSURE DATA

FREQ. (Hz)	HOT WIRE (volts)			TAP 22 (volts)			$\frac{P'_{22}}{P'_I}$	FIGURE
	mean	RMS	P'_I	mean	RMS	P'_{22}		
A. Maximum Plenum Pressure Amplitude:								
3.6	1.00	0.23	23%	1.45	0.10	6.89%	0.30	11
5.1	1.00	0.30	30%	1.47	0.085	5.78%	0.19	12
7.0	1.00	0.35	35%	1.48	0.07	4.73%	0.13	13
10.0	1.00	0.35	35%	1.51	0.07	4.64%	0.13	14
15.1	1.00	0.43	43%	1.55	0.07	4.52%	0.10	15
B. One-Half Maximum Plenum Pressure Amplitude:								
3.6	1.00	0.13	13%	1.60	0.07	4.38%	0.34	-
5.1	1.00	0.13	13%	1.60	0.06	3.59%	0.28	-
7.0	1.00	0.18	18%	1.66	0.06	3.61%	0.20	-
10.0	1.00	0.18	18%	1.69	0.06	3.55%	0.20	-
15.1	1.00	0.22	22%	1.70	0.06	3.53%	0.16	-

five evaluations are plotted in Fig. 17 along with the curve of C_L vs. C_μ for non-oscillating C_μ conditions.[3] This shows that oscillating C_μ about some mean value had very little effect on the mean value of C_L. Therefore, the curve of Fig. 17 is a transfer function between C_μ and C_L; knowing the maximum and minimum values of the fluctuating C_μ, it should be possible to predict the maximum and minimum values of the resulting C_L.

---

[3]The steady C_μ curve in Fig. 17 is from data previously taken by Prof. James Miller and Prof. Lou Schmidt of the Naval Postgraduate School, using the same equipment described in section II.

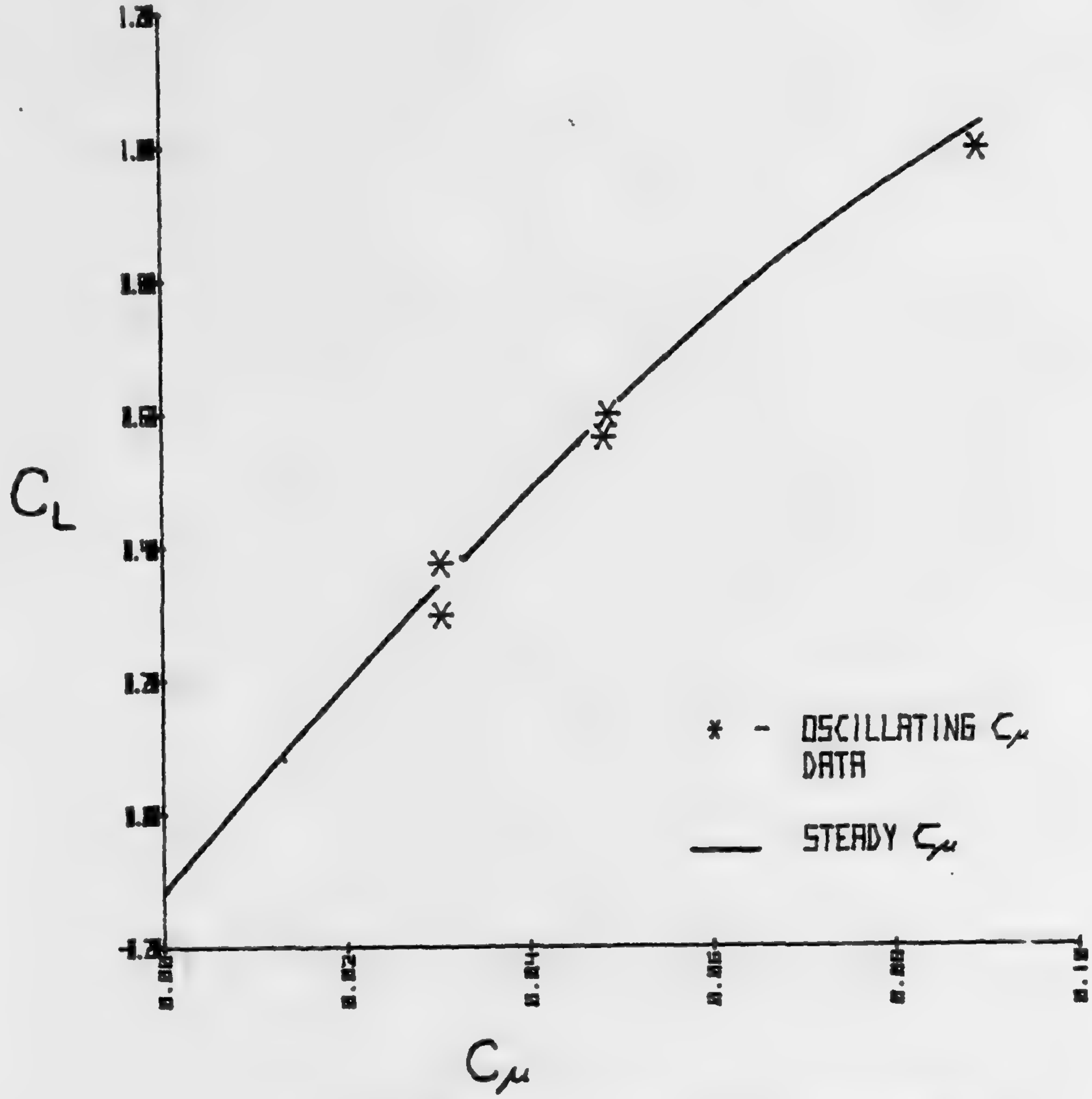

NOTE: Pressure tap data for the unsteady C_μ evaluations can be found in the Appendix.

Figure 17

Comparison of Mean Lift Coefficient Generated by Both Steady and Oscillating C_μ

IV. CONCLUSIONS

The objective of this investigation was two-fold: design and construct a simple control valve to generate an oscillating C_μ and evaluate the effect of this oscillating C_μ on the lift coefficient of the model.

The pressure wave created by the control valve was subject to substantial distortion under certain conditions, but it is believed this distortion was largely due to systemic effects. Evaluation of the valve output using a temporary installation much nearer the model failed to detect the distortion mentioned in section III. C. 2. The amplitude of the pressure wave was frequency dependent, increasing with higher frequency.

The second part of the investigation was not successful. As mentioned in section III. D., it was assumed at the outset of the evaluation that each of the pressure taps would show some oscillatory effect from the fluctuating C_μ. If this effect could have been recorded in terms of mean value, amplitude, and phase difference from the plenum pressure signal, the values from each of the 53 taps could have been used to construct a plot of the variation in C_L, C_D and C_m with plenum pressure. Since only a few of the taps showed any effects from the oscillating C_μ, this approach was not possible.

In order to find out why the pressure fluctuations did not propagate around the airfoil as anticipated, the model was closely examined and it was discovered that the slot width was not 0.010 inch across the entire span, but rather it varied considerably. In several places the slot was completely closed off. This undoubtedly had a large effect on the trailing edge jet wake and its subsequent effect on the pressure distribution about the model. The blockage of the slot also significantly reduced the total slot exit area, A_s, and therefore affected the ratio of slot exit area to maximum control valve area. Some pressure wave distortion may have been caused by this, if the ratio varied significantly from 1.0.

The conclusion, therefore, is that while the analysis of the control valve performance and plenum pressure fluctuations is considered to be accurate, the data pertaining to the exterior pressure variations are questionable and will require more investigation after the model is repaired.

APPENDIX

PRESSURE TAP MEAN VALUE DATA WITH OSCILLATING C_μ

Freq. = 28.6 Hz $\overline{C_\mu}$ = 0.0304 P'_I = 21% C_L = 0.375

Angle of attack = -5° q = 5.59 cm H_2O

TAP #	C_p	TAP #	C_p	TAP #	C_p
1	0.721	19	-0.802	37	-0.152
2	1.000	20	-0.783	38	-0.165
3	0.958	21	1.000 (1)	39	-0.098
4	0.778	22	-2.440	40	30.370 (1)
5	0.579	23	-0.147	41	-0.213
6	0.416	24	0.015	42	-0.301
7	0.057	25	-0.087	43	-0.422
8	-0.042	26	-0.136	44	-0.452
9	-0.314	27	0.008	45	-0.478
10	-0.397	28	-0.018	46	-0.432
11	-0.627	29	0.187	47	-0.668
12	-0.618	30	0.022	48	-0.763
13	-0.813	31	-0.045	49	-0.851
14	-1.958 (1)	32	-0.050	50	-0.416
15	-0.945	33	-0.095	51	-0.851
16	-0.940	34	-0.047	52	-0.316
17	-0.943	35	1.000 (1)	53	0.021
18	-0.875	36	-0.111		

(1) These four data points are in error due to leaks in the pressure leads. During data reduction, the pressure at these points was artificially changed to an average value of the pressures on either side.

PRESSURE TAP MEAN VALUE DATA WITH OSCILLATING C_μ

Freq. = 28.6 Hz $\quad \bar{C_\mu} = 0.0305 \quad P_I' = 41\% \quad C_L = 0.298$

Angle of attack = -5° $\quad q = 5.59$ cm H_2O

TAP #	C_P	TAP #	C_P	TAP #	C_P
1	0.868	19	-0.735	37	-0.135
2	1.002	20	-0.626	38	-0.158
3	0.938	21	1.000 (1)	39	-0.179
4	0.788	22	-2.413	40	30.288
5	0.541	23	-0.122	41	-0.227
6	0.451	24	0.018	42	-0.286
7	0.186	25	-0.125	43	-0.439
8	-0.020	26	-0.151	44	-0.464
9	-0.230	27	0.015	45	-0.423
10	-0.389	28	0.015	46	-0.536
11	-0.569	29	0.175	47	-0.584
12	-0.591	30	0.005	48	-0.712
13	-0.773	31	-0.015	49	-0.872
14	-2.090 (1)	32	-0.077	50	-0.617
15	-0.965	33	-0.117	51	-0.765
16	-0.915	34	-0.067	52	-0.505
17	-0.209	35	1.000 (1)	53	0.327
18	-0.873	36	-0.133		

(1) These four data points are in error due to leaks in the pressure leads. During data reduction, the pressure at these points was artificially changed to an average value of the pressures on either side.

PRESSURE TAP MEAN VALUE DATA WITH OSCILLATING C_μ

Freq. = 10.2 Hz $\bar{C_\mu}$ = 0.0483 P_I' = 22% C_L = 0.564

Angle of attack = -5° q = 5.59 cm H_2O

TAP #	C_P	TAP #	C_P	TAP #	C_P
1	0.894	19	-0.878	37	-0.128
2	0.894	20	-0.755	38	-0.144
3	0.943	21	1.000 (1)	39	-0.027
4	0.612	22	-3.572	40	35.614 (1)
5	0.486	23	-0.356	41	-0.205
6	0.173	24	-0.051	42	-0.271
7	-0.019	25	-0.213	43	-0.364
8	-0.264	26	-0.436	44	-0.362
9	-0.434	27	-0.152	45	-0.420
10	-0.625	28	0.101	46	-0.404
11	-0.691	29	0.010	47	-0.551
12	-0.811	30	-0.155	48	-0.689
13	-0.917	31	-0.214	49	-0.577
14	-2.935 (1)	32	-0.163	50	-0.285
15	-1.075	33	-0.194	51	-0.356
16	-1.057	34	-0.031	52	-0.138
17	-1.080	35	1.000 (1)	53	0.519
18	-0.990	36	-0.101		

(1) These four data points are in error due to leaks in the pressure leads. During data reduction, the pressure at these points was artificially changed to an average value of the pressures on either side.

PRESSURE TAP MEAN VALUE DATA WITH OSCILLATING C_μ

Freq. = 16.0 Hz $\overline{C_\mu}$ = 0.0488 P'_I = 30% C_L = 0.598

Angle of attack = -5° q = 5.59 cm H_2O

TAP #	C_P	TAP #	C_P	TAP #	C_P
1	0.982	19	-0.857	37	-0.122
2	0.982	20	-0.766	38	-0.124
3	0.927	21	1.000 (1)	39	-0.021
4	0.732	22	-3.608	40	35.325 (1)
5	0.484	23	-0.460	41	-0.185
6	0.245	24	-0.071	42	-0.291
7	-0.050	25	-0.206	43	-0.349
8	-0.198	26	-0.444	44	-0.365
9	-0.489	27	-0.164	45	-0.407
10	-0.643	28	0.103	46	-0.378
11	-0.746	29	-0.065	47	-0.410
12	-0.810	30	-0.096	48	-0.622
13	-0.987	31	-0.138	49	-0.577
14	-2.997 (1)	32	-0.242	50	-0.114
15	-1.122	33	-0.273	51	-0.172
16	-1.070	34	-0.003	52	0.016
17	-1.058	35	1.000 (1)	53	0.677
18	-1.003	36	-0.108		

(1) These four data points are in error due to leaks in the pressure leads. During data reduction, the pressure at these points was artificially changed to an average value of the pressures on eith side.

PRESSURE TAP MEAN VALUE DATA WITH OSCILLATING C_μ

Freq. = 5.0 Hz $\overline{C_\mu}$ = 0.0892 P'_I = 27% C_L = 0.996

Angle of attack = -5° q = 5.59 cm H_2O

TAP #	C_P	TAP #	C_P	TAP #	C_P
1	1.005	19	-1.109	37	-0.048
2	0.965	20	-1.183	38	-0.048
3	0.557	21	1.000 (1)	39	-0.056
4	0.428	22	-6.275	40	32.270 (1)
5	0.267	23	-0.758	41	-0.130
6	0.012	24	-0.422	42	-0.196
7	-0.163	25	-0.532	43	-0.247
8	-0.569	26	-0.779	44	-0.280
9	-0.723	27	-0.191	45	-0.260
10	-0.824	28	-1.417	46	-0.191
11	-1.046	29	-0.809	47	-0.285
12	-1.084	30	-0.136	48	-0.244
13	-1.223	31	-0.532	49	-0.384
14	-5.089 (1)	32	-0.265	50	0.003
15	-1.391	33	-0.356	51	0.043
16	-1.324	34	-0.050	52	0.522
17	-1.351	35	1.000 (1)	53	0.822
18	-1.307	36	-0.018		

(1) These four data points are in error due to leaks in the pressure leads. During data reduction, the pressure at these points was artificially changed to an average value of the pressures on either side.

LIST OF REFERENCES

1. Naval Ship Research and Development Center Technical Note AL-211, Two-Dimensional Subsonic Wind Tunnel Tests of Two 15-Percent Thick Circulation Control Airfoils, by-Robert J. Englar, August 1971.

2. Naval Ship Research and Development Center Technical Note AL-201, Two-Dimensional Subsonic Wind Tunnel Investigations of a Cambered 30-Percent Thick Circulation Control Airfoil, by Robert J. Englar, May 1972.

3. Naval Ship Research and Development Center Report 4070, Evaluation of a Pneumatic Valving System for Application to a Circulation Control Rotor, by Kenneth R. Reader, May 1973.

4. Lockheed - California Company Report LR 26417, Design Study of a Helicopter with a Circulation Control Rotor, by W. D. Anderson, and others, May 1974.

5. David W. Taylor Naval Ship Research and Development Center Report 76-0062, A Control System for the Wind Tunnel Model of a Reverse Blowing Circulation Control Rotor, by Kenneth R. Reader, p. 28, May 1976.